

# Synthesis and characterisation of a novel mixed donor P,O,P' nixantphos ligand and its metal complex



Thashree Marimuthu, Muhammad D. Bala\*, Holger B. Friedrich\*\*

School of Chemistry & Physics, University of KwaZulu-Natal, Private Bag X54001, Durban 4000, South Africa

## ARTICLE INFO

### Article history:

Received 4 August 2015

Received in revised form

23 October 2015

Accepted 26 October 2015

Available online 30 October 2015

### Keywords:

Nixantphos

Iridium complex

Bite angle

Catalyst

## ABSTRACT

The complex  $[(\text{NixC8OH})\text{Ir}(\text{cod})\text{Cl}]$  **4** has been synthesized and structurally characterized by NMR, IR and single crystal X-ray diffraction. The synthesis and characterisation of the novel ligand NixC8OH is also presented. The coordination around Ir is trigonal bipyramidal with both P groups of the NixC8OH ligand bound in a *bis*-equatorial mode. The *bis*-chelating cod ( $\text{C}_8\text{H}_{12}$ ) ligand occupies the remaining equatorial position and an axial position. This mode of bonding has resulted in a large bite angle (P1–Ir–P2) of  $102.92(12)^\circ$  for the title complex **4**. The IR and NMR data further support the elucidated structure. Thermal analyses of **4** indicate that it is thermally stable up to a decomposition temperature of  $>400^\circ\text{C}$ .

© 2015 Elsevier B.V. All rights reserved.

## 1. Introduction

The ability to control the shape of a coordination compound in catalysis has been an area of intense research interest. The pioneering work of Trofimenko in the mid 1960's introduced *tris*-(pyrazol-1-yl)borate anions (Tp) and their analogues into the field of coordination chemistry [1–4]. These ligands were characterised by their unique *fac* binding (Fig. 1a) to a metal centre and are known as scorpionate ligands. Other tridentate ligands including the pincer types preferentially coordinate to metals in a *mer* binding mode (Fig. 1b). Additionally, PCP pincer ligands due to the disposition of their donor atoms give complexes with Ir that can activate highly inert C–H bonds [5]. Based on the success of tridentate ligands we became interested in the design and complexation of a new class of xanthene based ligands.

Herein we report the synthesis of a mixed donor P,O,P' scorpionate type ligand **2** and the structure of its iridium metal complex **4** (Scheme 1). The ligand backbone nixantphos **1** belongs to the xanthene family introduced by van Leeuwen and co-workers [7,8]. These ligands have been extensively reviewed for their P,P *cis*- $\kappa^2$  coordination mode to transitional metal centres [9–14] (Fig. 1c),

and some fully characterised cationic and neutral complexes exhibiting *mer*- $\kappa^3$ -P,O,P coordination modes via the oxygen atom of the xanthene ring have been reported (Fig. 1b) [15–22]. It is important to highlight that recently Weller and co-workers have reported the structure of the complex  $[\text{Ir}(\kappa^3(\text{Xantphos})(\text{H})(\mu\text{-H}))_2[\text{BAR}^F_4]_2]$  which also displayed the rare *fac*- $\kappa^3$ -P,O,P coordination [15]. This study, therefore serves as another basis towards the unambiguous preparation of *fac* coordinating  $\kappa^3$  ligands derived from nixantphos **1** where a third donor has been functionalised onto the backbone.

## 2. Experimental

### 2.1. Materials and methods

Chemicals used were of reagent grade and reactions were carried out in distilled and dried solvents using standard Schlenk tube techniques under inert and dry nitrogen atmosphere. Iridium trichloride hydrate ( $\text{IrCl}_3 \cdot x\text{H}_2\text{O}$ ) was obtained from Johnson Matthey and used as received. The precursor (8-bromooctyloxy)(*t*-butyl)dimethylsilane was prepared by literature method [23]. The dimeric chloro bridged precursor di- $\mu$ -bis(1,5-cyclooctadiene) diiridium(I)  $[\text{Ir}(\text{cod})\text{Cl}]_2$  **2** was prepared by the reduction of  $\text{IrCl}_3$  in the presence of excess 1,5-cyclooctadiene (cod) (Fluka  $\geq 98\%$ ) in aqueous ethanol (Merck absolute ACS grade) [24]. FTIR spectra were recorded in the  $4000\text{--}400\text{ cm}^{-1}$  region on a Perkin Elmer attenuated total reflectance (ATR) infrared spectrophotometer.  $^1\text{H}$ ,

\* Corresponding author.

\*\* Corresponding author.

E-mail addresses: [bala@ukzn.ac.za](mailto:bala@ukzn.ac.za) (M.D. Bala), [friedric@ukzn.ac.za](mailto:friedric@ukzn.ac.za) (H.B. Friedrich).

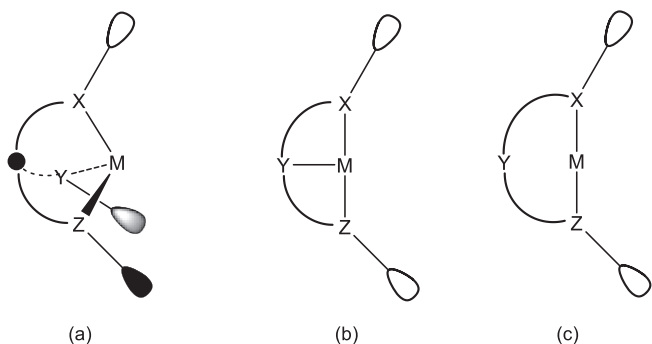
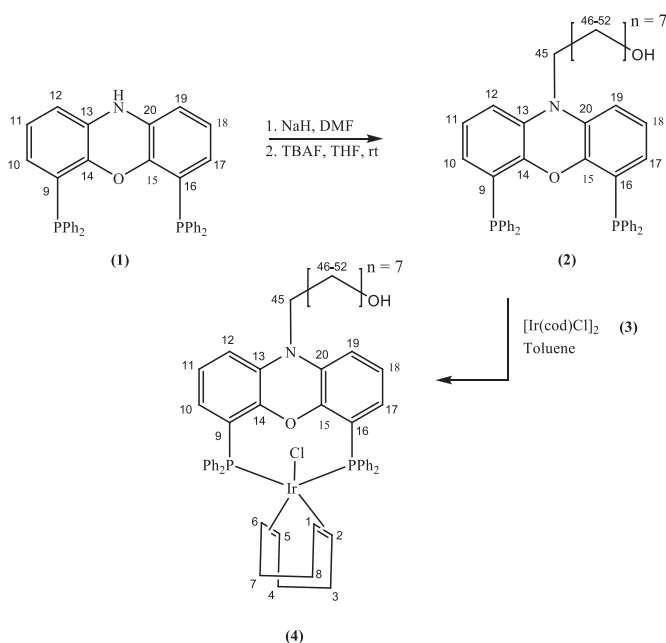


**Fig. 1.** Comparison between (a) the *fac* coordination of a  $\kappa^3$  tripodal ligand (b) the *mer* binding of a  $\kappa^3$  pincer ligand and (c) *cis*- $\kappa^2$  coordination of a bidentate ligand [6].



**Scheme 1.** Synthesis of the title complex **4** from ligand **2**.

$^{31}\text{P}$  and  $^{13}\text{C}$  NMR measurements were collected at 298 K with Bruker AVANCE III 400 MHz and 600 MHz spectrometers using 5 mm tubes and deuterated chloroform as the solvent. Coupling constants ( $J$ ) are given in Hz. The melting point was determined using a Gallenkamp melting point apparatus and is uncorrected. High resolution mass spectroscopy was obtained with the Bruker micrOTOF-Q II instrument operating at ambient temperatures, under electron spray ionisation conditions (ESI), using a sample concentration of approximately 1 ppm. Differential scanning calorimetry (DSC) measurements ( $\text{Al}_2\text{O}_3$  reference standard) were performed on a TA Thermo Gravimetric Analyser at a heating rate of  $10^\circ\text{C}/\text{min}$  under nitrogen atmosphere. Elemental analyses were performed on a LECO CHNS-932 elemental analyser.

### 2.1.1. Synthesis of compounds **2** and **4**

Synthesis of **2**. Nixantphos **1** (200 mg, 0.36 mmols) was dissolved in DMF (4 mL). To the orange reaction mixture, NaH (400 mg, 0.72 mmol) was added. (8-bromooctyloxy)(*t*-butyl)dimethylsilane (180 mg, 0.63 mmol) was slowly added, and the mixture stirred at  $100^\circ\text{C}$  overnight. The reaction was worked up by the addition of water (10 mL) and the organic phase extracted with ethyl acetate

( $4 \times 10$  mL). The collective fractions were dried over anhydrous sodium sulphate and purified by column chromatography with 10% hexane/ethyl acetate elution. The resulting oil was dissolved in THF (25 mL), and tetra-*N*-butylammonium fluoride added and solution was left to stir overnight at room temperature. Thereafter, similar aqueous work-up was carried out. The crude product was purified by column chromatography with 20% ethyl acetate/hexane elution to afford **2** in 28% (38 mg oil). IR  $\nu_{\text{max}}$  ( $\text{cm}^{-1}$ ): 3343(m), 3053(m), 2924(m), 2853(m), 1726(m), 1462(s), 1435(s), 1412(s), 1276(m), 1222(m), 743(s), 693(s); HR-MS (ESI) ( $m/z$ ):  $[\text{M}+\text{H}]^+$  calcd. for  $\text{C}_{44}\text{H}_{44}\text{NO}_2\text{P}_2$ , 680.2842; found, 680.2843. Details of the NMR data are presented in Table 1.

Synthesis of **4**. Compound **3** (30 mg, 0.04 mmol) was added to  $[\text{Ir}(\text{cod})\text{Cl}]_2$  (13.4 mg, 0.02 mmol) in THF (6 mL) under an inert argon atmosphere at room temperature. Immediate discoloration was observed, and the mixture was allowed to stir overnight. The THF solvent was removed *in vacuo* and the resulting precipitate was washed with hexane ( $3 \times 6$  mL), and extracted with dichloromethane ( $2 \times 6$  mL). The dichloromethane was removed *in vacuo* and the complex **4** dried under high vacuum overnight to afford **4** in 52% (21 mg yellow powder). Melting point 504 K, DSC 513 K; IR  $\nu_{\text{max}}$  ( $\text{cm}^{-1}$ ): 1938(s), 2920(m), 1585(m), 1489(s); HRMS (ESI) ( $m/z$ ):  $[\text{M}]^+ - \text{Cl}$  calcd for  $\text{C}_{52}\text{H}_{55}\text{IrNO}_2\text{P}_2$ , 980.3332; found, 980.3333; EA: Calculated for  $\text{C}_{52}\text{H}_{55}\text{ClIrNO}_2\text{P}_2$ : C, 61.5; H, 5.5; N, 1.4. Found: C, 61.0; H, 5.2; N, 1.3. Details of NMR data are presented in Table 2.

### 2.1.2. Structure analysis and refinement

Single-crystal structure determination by X-ray diffraction was performed on a Bruker APEXII CCD area-detector diffractometer with graphite monochromated  $\text{Mo } K_\alpha$  radiation (50 kV, 30 mA) using the APEX 2 data collection software [25]. The collection method involved  $\omega$ -scans of width  $0.5^\circ$  and  $512 \times 512$  bit data frames. Data reduction was carried out using the SAINT+ software [26] and face indexed absorption corrections were made using the software XPREP. The crystal structure was solved by direct methods using SHELXTL. Non-hydrogen atoms were first refined isotropically followed by anisotropic refinement by full matrix least-squares calculations based on  $F^2$  using SHELXTL. Hydrogen atoms were first located in the difference map then positioned geometrically and allowed to ride on their respective parent atoms with  $\text{C}-\text{H} = 0.95 \text{ \AA}$  and  $U_{\text{iso}}(\text{H}) = 1.2U_{\text{eq}}(\text{C})$ . Diagrams and publication material were generated using SHELXTL [27], PLATON [28] and ORTEP-3 [29]. The *n*-octanol tail was found to be disordered. As a consequence it was refined over two positions with final occupancies of 0.414(14) and 0.586(14) using SADI restraints. Further details of the X-ray structural analysis are given in Table 3, while selected bond lengths and angles for **4** are listed in Table 4. The asymmetric unit was found to contain 2 molecules and 1 fragment of 2-propanol.

## 3. Results and discussion

### 3.1. Synthesis

Ligand **2** was prepared by the sodium hydride induced alkylation of nixantphos **1** with a protected tail precursor. Deprotection by standard methods of the resulting product resulted in the O-donor ligand **2**. Complex **4** was readily prepared from  $[\text{Ir}(\text{cod})\text{Cl}]_2$  metal precursor and ligand **2** at room temperature to afford 52% yield of a yellow powder. Single crystals of **4** suitable for X-ray analyses were grown by slow diffusion of 2-propanol into a dichloromethane solution of the complex.

**Table 1**  
NMR spectroscopic data for **2**.

| <sup>a</sup> Carbon number | <sup>1</sup> H ( $\delta$ = ppm) | <sup>13</sup> C ( $\delta$ = ppm)   |
|----------------------------|----------------------------------|---|
| 12, 19                     | 6.4 bd [ $J$ (H,H) = 7.8]        | 111.7   |
| 11, 18                     | 6.6 t [ $J$ (H,H) = 7.8]         | 123.5   |
| 10, 17                     | 6.0 m                            | 125.1   |
| C46–C51                    | 1.6–1.2(12H)                     | 32.7, 29.4, 29.4, 26.9, 25.7, 24.7  |
| C46                        | 3.6 [t, $J$ = 6.5 Hz]            | 63.0  |
| C52                        | 3.5 [t, $J$ = 7.8 Hz]            | 44.7  |
| Phenyl groups on P1 & P2   | 7.5–7.1 m (20H)                  | 128.1 t, [ $J$ (P,C) = 3.4 Hz],<br>133.9 d, [ $J$ (P,C) = 10.3 Hz], 128.2 m |
| C14,15                     | –                                | 147.1 m   |
| C21,31,41,51               | –                                | 137.0 t, [ $J$ (P,C) = 6.5 Hz]  |
| C13,20                     | –                                | 133.2 t, [ $J$ (P,C) = 1.8 Hz]  |
| C9,16                      | –                                | 124.8 d, [ $J$ (P,C) = 6.3 Hz]  |

<sup>a</sup> Carbon numbers relative to the numbering scheme for **2** in Scheme 1.**Table 2**  
NMR spectroscopic data for **4**.

| <sup>a</sup> Carbon number | <sup>1</sup> H ( $\delta$ = ppm) | <sup>13</sup> C ( $\delta$ = ppm)  |
|----------------------------|----------------------------------|--|
| 12, 19                     | 6.6 bd [ $J$ (H,H) = 7.8]        | 112.6  |
| 11, 18                     | 6.8 t [ $J$ (H,H) = 7.9]         | 123.5 t, [ $J$ (P,C) = 2.5 Hz]   |
| 10, 17                     | 6.2 m (2H)                       | 125.0  |
| C46–C51 and 3, 4, 7, 8     | 1.8–1.3 m (8H, 12H)              | 27.0, 25.6, 25.5, 24.5, 29.3, 29.3<br>29.2   |
| C45                        | 3.6 t [ $J$ (H,H) = 7.8 Hz]      | 63.0   |
| C52                        | 3.6 t [ $J$ (H,H) = 6.5 Hz]      | 44.2   |
| 1, 2, 5, 6                 | 3.4 bs 4H                        | 63.1 m   |
| Phenyl groups on P1 & P2   | 7.6–7.2 m (12H), 7.1–7.0 (8H)    | 133.9 t, [ $J$ (P,C) = 5.2 Hz], 128.9 d, [ $J$ (P,C) = 24.4 Hz], 128.1 (t, [ $J$ (P,C) = 8 Hz] |
| C14,15                     | –                                | 147.8 t [ $J$ (P,C) = 9Hz]   |
| C21,31,41,51               | –                                | 137.7 dd, [ $J$ (P,C) = 38.6, 2.8 Hz]  |
| C13,20                     | –                                | 132.8 dd, [ $J$ (P,C) = 31.1, 5.6 Hz]  |
| C9,16                      | –                                | 120.7 dd, [ $J$ (P,C) = 37.4, 5.3 Hz]  |

<sup>a</sup> Carbon numbers relative to the numbering scheme for **4** in Scheme 1.**Table 3**  
Crystal data and structure refinement parameters for **4**.

|                                   |  |
|-----------------------------------|--|
| Empirical formula                 | C <sub>54</sub> H <sub>60</sub> ClIrNO <sub>4</sub> P <sub>2</sub> |
| Formula weight                    | 1124.68  |
| Crystal system                    | Triclinic  |
| Space group                       | P-1  |
| a = 12.4659(7) Å                  | $\alpha$ = 98.836(5)°  |
| b = 12.6172(8) Å                  | $\beta$ = 99.860(6)°   |
| c = 18.2748(16) Å                 | $\gamma$ = 111.390(4)°   |
| Volume                            | 2562.6(3) Å <sup>3</sup>   |
| Z                                 | 2  |
| Density (calculated)              | 1.355 Mg/m <sup>3</sup>  |
| Absorption coefficient            | 2.758 mm <sup>-1</sup>   |
| F(000)                            | 1064   |
| Reflections collected             | 14,310   |
| Independent reflections           | 11,770 [R(int) = 0.1169]   |
| Goodness-of-fit on F <sup>2</sup> | 1.175  |
| Final R indices [I > 2sigma(I)]   | R1 = 0.1234, wR2 = 0.1924  |
| R indices (all data)              | R1 = 0.2214, wR2 = 0.2205  |

**Table 4**  
Bond lengths [Å] and angles [°] for **4**.

|                 |           |                  |            |
|-----------------|-----------|------------------|------------|
| C(45)–N(1)      | 1.496(12) | C(2)–Ir(1)–P(1)  | 152.0(4)   |
| C(9)–P(1)       | 1.845(12) | C(6)–Ir(1)–P(1)  | 81.9(5)    |
| C(14)–O(1)      | 1.405(14) | C(5)–Ir(1)–P(1)  | 107.9(5)   |
| C(15)–O(1)      | 1.335(19) | C(2)–Ir(1)–Cl(1) | 85.0(4)    |
| C(13)–N(1)      | 1.406(17) | C(1)–Ir(1)–Cl(1) | 84.0(5)    |
| C(1)–Ir(1)      | 2.113(17) | C(6)–Ir(1)–Cl(1) | 155.5(4)   |
| C(2)–Ir(1)      | 2.105(17) | C(5)–Ir(1)–Cl(1) | 162.5(4)   |
| C(5)–Ir(1)      | 2.152(13) | P(1)–Ir(1)–Cl(1) | 89.11(12)  |
| C(6)–Ir(1)      | 2.201(12) | P(1)–Ir(1)–P(2)  | 102.92(12) |
| Cl(1)–Ir(1)     | 2.408(3)  | Cl(1)–Ir(1)–P(2) | 87.01(11)  |
| Ir(1)–P(1)      | 2.387(4)  | C(20)–N(1)–C(13) | 119.3(11)  |
| Ir(1)–P(2)      | 2.469(3)  | C(14)–O(1)–C(15) | 114.7(9)   |
| C(52A)–O(2A)    | 1.70(3)   | C(9)–P(1)–Ir(1)  | 118.0(4)   |
| C(1)–Ir(1)–P(1) | 113.1(5)  | C(16)–P(2)–Ir(1) | 117.8(4)   |

observed in the <sup>31</sup>P NMR, indicating that the two diphosphorus atoms were in a chemically equivalent environment.

### 3.2. NMR data

#### 3.2.1. Ligand **2**

The NMR data for the free ligand prepared is presented in Table 1. The signals at 6.4 ppm, 6.6 ppm and 6.0 ppm were assigned to the neighbouring protons of the phenoxazine ring. The splitting pattern and coupling constant was similar to reported nixantphos [30]. A methylenic triplet at 3.6 and a triplet at 3.5 ppm for the protons C46 and C52 were indicative of the functionalisation of the amine with the n-octanol tail. The corresponding signals in the <sup>13</sup>C NMR were at  $\delta$  = 63 and 44.7 ppm respectively. The multiplets between 1.6 and 1.2 integrating for 12 protons were assigned to the remaining six methylene groups. A singlet at –19.2 ppm was

#### 3.2.2. Complex **4**

The structure of complex **4** can be described as symmetrical about a mirror plane that bisects the molecule through the N...O...Ir...Cl vector. This renders the positions at carbons 12 & 19, 11 & 18 and 10 & 17 on the nixantphos ligand chemically equivalent as shown in Table 1. Also carbon positions on the cod ligand in chemically equivalent positions are summarised in Table 1. The neighbouring protons on the backbone of the coordinated ligand exhibit slight downfield shifts in both proton and carbon NMR in comparison to the chemical shifts of free **2** (Table 1). According to HH (COSY), H<sup>12,19</sup> coupled with H<sup>11,18</sup> corresponding to a broad doublet at 6.6 ppm (d,  $J$ (H,H) = 7.8 Hz); and H<sup>11,18</sup> coupled with

$H^{12,19}$  and  $H^{10,17}$  corresponding to a triplet at 6.8 ppm (t,  $J(H,H) = 7.9$  Hz); and a multiplet at 6.2 ppm due to a ABCXX'' system ( $X$  and  $X'' = {}^{31}P$ ) for  $H^{10,17}$ . In the  ${}^1H$  NMR spectrum, the olefinic proton of the coordinated cod is a broad singlet at 3.4 ppm, implying that these protons are in chemically equivalent environments. The corresponding signal appeared at 63.1 ppm in the HSQC spectrum and lies in the region typical of bound alkene ligands. The signal for the methylenic protons of the cod (Table 2) overlapped with that for the methylenic protons of the alkyl chain, and the multiplets between 1.7 and 1.2 ppm integrated for 20 protons. A single peak was observed in the  ${}^{13}C$  NMR spectrum at 29.2 ppm ( $CH_2$ ), assigned to C3, C4, C7, and C8. In the  ${}^1H$  NMR spectrum, a triplet at 3.6 was assigned to the proton of the  $-CH_2OH$  group of the n-octanol tail and correlated with a carbon at  $\delta$  63.0 ppm in the HSQC spectrum. Both signals showed no difference in chemical shift, compared to the free ligand and this is indicative of the uncoordinated O donor. The six remaining carbons on the alkyl tail were assigned to the signals at 27.0, 25.6, 25.5, 24.5, 29.3, 29.3 ppm.

For the carbons directed bonded to phosphorus atoms, a doublet of doublets with larger coupling constants compared to the free ligand is observed. The largest upfield shift is found for the ipso carbon of the phenyl and phenoxazine ring upon coordination. The coordination shift is less pronounced on going from the ipso to para carbon of the phenyl rings. For example C13,20 at  $\delta = 133.2$  ppm (Table 1) shifted up-field to  $\delta = 132.8$  ppm (Table 2), whereas the signal for the ortho carbons C21,31,41,51 only slightly moved from  $\delta = 137.7$  ppm (Table 1) to  $\delta = 137.0$  ppm (Table 2). Therefore the difference in the chemical shifts between the free ligand and coordinated ligand depends on the position of the carbon atom relative to the phosphorus atom. The shielding of the aromatic carbons is due to an increase in the  $\pi$ -electron density in the ring upon coordination, as the involvement of the phosphorus atom to the phenyl ring  $\pi$ -delocalization is reduced by the M–P back bonding. When the diphosphine ligand coordinates to the metal, the empty d-orbitals on the phosphorus atoms accept  $\pi$ -electron density from the filled metal d-orbitals. This additional electron density is then channelled into the phenyl ring and ligand backbone through the  $2\pi-d\pi$  interactions [31,32]. This increase in delocalization results in the observed up-field shifts of the phenyl carbon atoms in the coordinated diphosphine. Analysis of the  ${}^{31}P$  NMR data shows that the coordinated phosphines exhibit a slight downfield shift (1.1 ppm) compared to the free ligand 2 suggesting coordination. The peak was observed as a singlet at  $-18.1$  ppm, indicating that the two phosphines reside in similar environment, i.e. both are equatorial as confirmed by the single crystal X-ray analysis (see below).

### 3.3. Mass spectroscopy (high resolution), elemental and DSC (differential scanning calorimeter) thermal analysis

The exact mass for 4 was calculated as 980.3332. The loss of the labile Cl ligand results in the positively charged adduct  $[Ir(cod)(NixC8OH)]^+$ . The mass spectrum of 4 show the highest intensity molecular peak at 980.3333  $m/z$  together with several isotopic peaks, from 977.3170 to 983.3385  $m/z$  with adjacent peaks separated by 1  $m/z$ . The observed isotope distribution pattern shows an envelope of peaks, which is characteristic of a monocation [33]. The pattern, also agrees well with the theoretical pattern and that found for reported  $[Ir(cod)(nixantphos)]^+$  complex [34]. The elemental analysis results (see the experimental section) are indicative of good bulk purity of the complex. The DSC revealed an exotherm representing crystallisation at 200 °C, followed by the melting point of 4 observed as an endotherm at 240 °C. The DSC results indicate that the complex has good thermal stability with the onset of decomposition at temperature  $>400$  °C.

### 3.4. IR data

The IR analysis of complex 4 confirmed the presence of a broad OH band at  $3411\text{ cm}^{-1}$  and a C–O absorption band near  $1027\text{ cm}^{-1}$  indicative of a primary alcohol. The diagnostic C=C and CH (cod) stretching bands were at 3055, 3010, and bending vibrations 2926, 2853 and  $2853\text{ cm}^{-1}$  were for both methylene groups for the alkyl tail and for the cod ligand. The aromatic C–C stretch bands (for the phenyl ring carbon bonds) appear at 1584, 1615, and  $1554\text{ cm}^{-1}$ . The bands for C–H bends appear around  $1000\text{ cm}^{-1}$  for the in-plane bends and about  $695\text{ cm}^{-1}$  for the out-of-plane bend.

### 3.5. X-ray diffraction data

Analysis of the single-crystal X-ray data confirmed the formation of the complex 4 and the preferred mode of coordination.

A simplified (for clarity) ORTEP representation of 4 is presented in Fig. 2 where the coordination of ligands around Ir is described as approximately trigonal bipyramidal when the cod ligand, the bis-phosphino chelated ligand 2 and the Cl atom are considered. This coordination essentially comprises of the equatorial plane and two axial planes. The equatorial plane contains the two *cis* phosphines (P1 and P2) and one cod double bond (C1=C2), while the two axial positions contain the second cod double bond (C5=C6) and the chloro ligand in *trans* positions. The P–Ir–P bond angle of  $102.92(12)^\circ$  is slightly smaller to that of  $[Ir(nixantphos)(cod)Cl]$

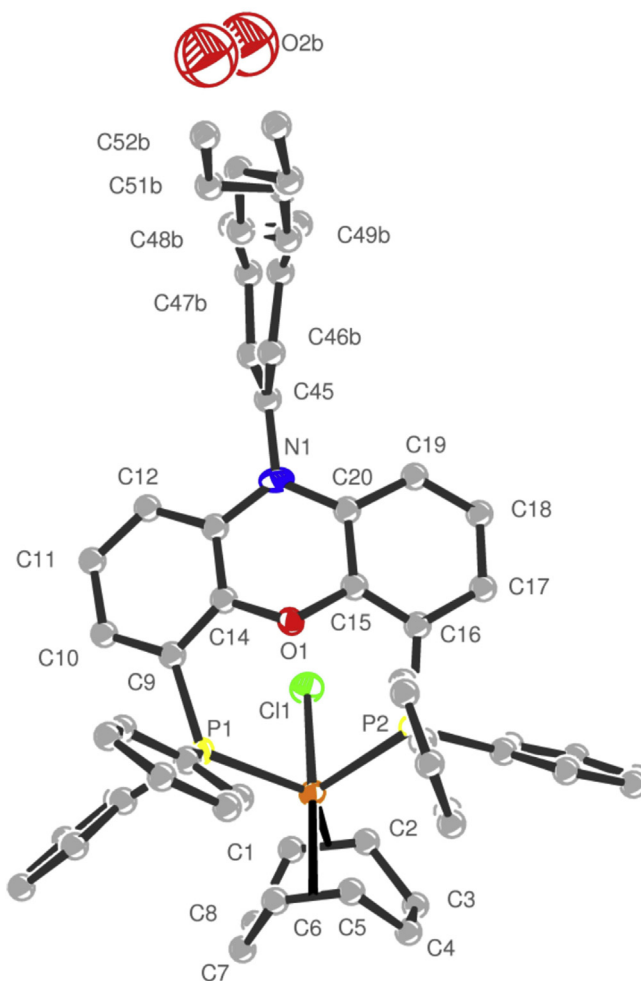


Fig. 2. ORTEP drawing of 4 showing the atom numbering scheme. Thermal ellipsoids are shown at 50% probability with hydrogen atoms omitted for clarity.

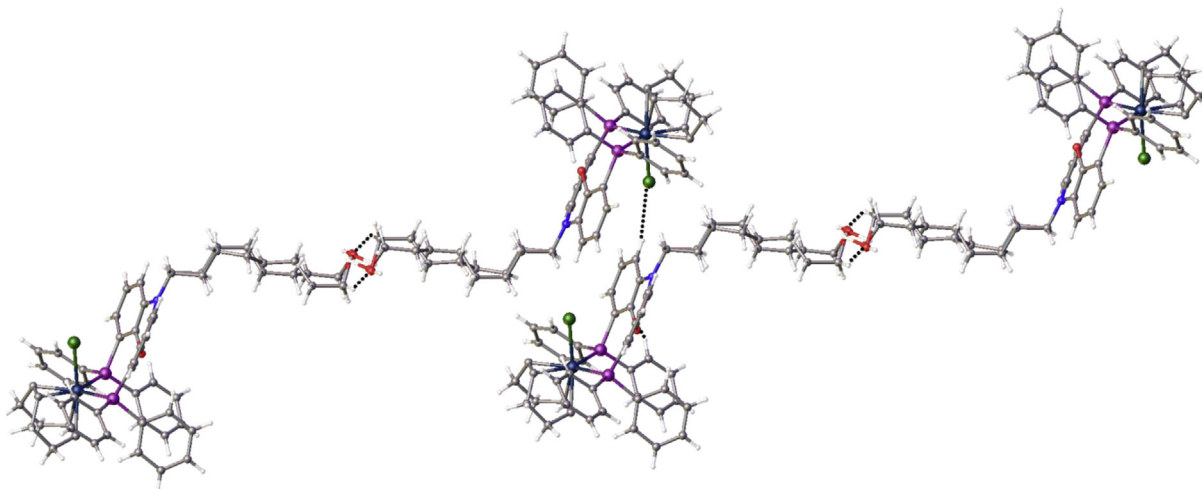


Fig. 3. Crystal packing in a molecule of **4** as seen along the *a* axis highlighting the C(12)-H(12)···Cl(1) inter-molecular interaction.

(106.49(3)°) [34] possibly due to the strain of the alkyl tail but comparable to [Ir(xantphos)(cod)][BAr<sup>F</sup><sub>4</sub>] (101.22(3)°) [15]. Considering a mean plane of planarity involving the 14 ring atoms of the ligand **2** it can be concluded that **4** is slightly bent about an N1–O1 axis in order to accommodate added strain due to Ir metal coordination. The uncoordinated and related ligand 6-[4,6-bis(diphenyl-phosphino)-10H-phenoxazin-10-yl]-hexan-1-ol is essentially planar [35]. However, the heteroatoms N1 and O1 respectively show deviations from planarity of 0.374(2) and 0.637(2) Å resulting in a strained backbone, this observation is similar to the reported [Ir(nixantphos)(cod)Cl] complex [34].

Several inter-molecular interactions are observed for the crystal structure of **4** (Fig. 3). The interactions C(12)-H(12)···Cl(1) possibly help stabilise the packing of the molecules. Similar interactions were reported for the [Ru(xantphos)(S-dmso)Cl<sub>2</sub>] complex [16].

Further stabilization of the crystal structure is afforded by O–H···O hydrogen bonding between the hydroxyl group of the *n*-octanol tail and the solvent (2-propanol) molecule.

#### 4. Conclusions

The novel mixed donor P,O,P' iridium complex has been synthesized and fully characterized. Coordination around Ir has been confirmed by NMR and single-crystal X-ray diffraction to be trigonal bipyramidal with both P groups of the NixC8OH bound equatorially.

#### Acknowledgements

We wish to thank Dr. Manuel Fernandes (University of the Witwatersrand) for crystal data collection, SASOL, THRIP and the University of KwaZulu-Natal for financial support. We gratefully acknowledge Johnson Matthey for a loan of iridium trichloride.

#### Appendix A. Supplementary material

Crystallographic data for the structures in this article have been deposited with the Cambridge Crystallographic Data Centre, CCDC 1403370. These data can be obtained free of charge at <http://www.ccdc.cam.ac.uk/conts/retrieving.html> (or from the Cambridge Crystallographic Data Centre, 12 Union Road Cambridge CB2 1EZ, UK; Fax: +44-1223/336-033; E-mail: [deposit@ccdc.cam.ac.uk](mailto:deposit@ccdc.cam.ac.uk)).

#### References

- [1] S. Trofimenko, *J. Am. Chem. Soc.* 89 (1967) 3904.
- [2] S. Trofimenko, *Acc. Chem. Res.* 4 (1971) 17.
- [3] S. Trofimenko, *Chem. Rev.* 72 (1972) 497.
- [4] S. Trofimenko, *Chem. Rev.* 93 (1993) 943.
- [5] J. Choi, A.H.R. MacArthur, M. Brookhart, A.S. Goldman, *Chem. Rev.* 111 (2011) 1761.
- [6] G. Parkin, *Chem. Commun.* (2000) 1971.
- [7] L.A. van der Veen, P.H. Keeven, G.C. Schoemaker, J.N.H. Reek, P.C.J. Kamer, P. van Leeuwen, M. Lutz, A.L. Spek, *Organometallics* 19 (2000) 872.
- [8] M. Kranenburg, Y.E.M. Vanderburgt, P.C.J. Kamer, P.W.N.M. van Leeuwen, K. Goubitz, J. Fraanje, *Organometallics* 14 (1995) 3081.
- [9] P.C.J. Kamer, P.W.N.M. van Leeuwen, *Acc. Chem. Res.* 34 (2001) 895.
- [10] P.W.N.M. van Leeuwen, P.C.J. Kamer, J.N.H. Reek, P. Dierkes, *Chem. Rev.* 100 (2000) 2741.
- [11] M.-N.B. Gensow, Z. Freixa, P.W.N.M. van Leeuwen, *Chem. Soc. Rev.* 38 (2009) 1099.
- [12] Z. Freixa, P.W.N.M. van Leeuwen, *Coord. Chem. Rev.* 252 (2008) 1755.
- [13] P.W.N.M. van Leeuwen, *Homogeneous Catalysis: Understanding the Art*, Kluwer Academic Publishers, Dordrecht, 2004.
- [14] D.K. Dutta, B. Deb, *Coord. Chem. Rev.* 255 (2011) 1686.
- [15] A.J. Pontiggia, A.B. Chaplin, A.S. Weller, *J. Organomet. Chem.* 696 (2011) 2870.
- [16] A.N. Kharat, A. Bakhoda, B.T. Jahromi, *Inorg. Chem. Commun.* 14 (2011) 1161.
- [17] A.E.W. Ledger, A. Moreno, C.E. Ellul, M.F. Mahon, P.S. Pregosin, M.K. Whittlesey, J.M.J. Williams, *Inorg. Chem.* 49 (2010) 7244.
- [18] L.D. Julian, J.F. Hartwig, *J. Am. Chem. Soc.* 132 (2010) 13813.
- [19] M.A. Zuidveld, B.H.G. Swennenhuis, M.D.K. Boele, Y. Guari, G.P.F. van Strijdonck, J.N.H. Reek, P.C.J. Kamer, K. Goubitz, J. Fraanje, M. Lutz, A.L. Spek, P.W.N.M. van Leeuwen, *J. Chem. Soc. Dalton Trans.* (2002) 2308.
- [20] P. Nieczypor, P.W.N.M. van Leeuwen, *J. Chem. Soc. Dalton Trans.* (2002) 2308.
- [21] A.J. Sandee, L.A. van der Veen, J.N.H. Reek, P.C.J. Kamer, M. Lutz, A.L. Spek, P.W.N.M. van Leeuwen, *Angew. Chem. Int. Ed.* 38 (1999) 3231.
- [22] G. Asensio, A.B. Cuenca, M.A. Esteruelas, M. Medio-Simon, M. Olivan, M. Valencia, *Inorg. Chem.* 49 (2010) 8665.
- [23] R.C. Gadwood, I.M. Mallick, A.J. Dewinter, *J. Org. Chem.* 52 (1987) 774.
- [24] G.W. Parshall, *Inorganic Synthesis*, McGraw-Hill, New York, 1974.
- [25] Bruker, APEX2 Version 2.0–1, Bruker AXS Inc., Madison, Wisconsin, USA, 2005.
- [26] Bruker, SAINT-NT. Version 6.0. (Includes XPREP and SADABS), Bruker AXS Inc., Madison, Wisconsin, USA, 2005.
- [27] G.M. Sheldrick, *Acta Cryst. A* 64 (2008) 112.
- [28] A.L. Spek, *J. Appl. Cryst.* 36 (2003) 7.
- [29] L.J. Farrugia, *J. Appl. Cryst.* 30 (1997) 565.
- [30] T. Marimuthu, M.D. Bala, H.B. Friedrich, *Acta Crystallogr. E* 64 (2008) O711.
- [31] Z. Ozer, S. Ozkar, *Turk. J. Chem.* 23 (1999) 9.
- [32] A.N. Hughes, D. Kleemola, *J. Heterocycl. Chem.* 13 (1976) 1.
- [33] W. Henderson, J.S. McIndoe, *Mass Spectroscopy of Inorganic, Coordination and Organometallic Compounds*, Wiley, Chichester, West Sussex, England, 2005.
- [34] T. Marimuthu, M.D. Bala, H.B. Friedrich, *J. Coord. Chem.* 62 (2009) 1407.
- [35] T. Marimuthu, M.D. Bala, H.B. Friedrich, *Acta Crystallogr. E* 64 (2008) O1984.